Role of eddies in cooling the Leeuwin Current

Catia M. Domingues,[1,2] Susan E. Wijffels,[1] Mathew E. Maltrud,[3] John A. Church,[1] and Matthias Tomczak[2]

Received 12 November 2005; revised 18 January 2006; accepted 23 January 2006; published 2 March 2006.

[1] The poleward flow of the Leeuwin Current dominates the surface circulation off Western Australia. Along its path, it cools by about 5°C over 1350 km. Based on an eddy permitting simulation using the Parallel Ocean Program model, we find that 70% of the heat advected into the coastal region off Western Australia by the narrow mean jet is transferred to the ocean interior through eddy heat fluxes. The eddy fluxes are associated with processes operating at submonthly timescales and despite the current's clear seasonal variability, seasonal rectification plays little role in the mean heat balance. The 43 TW transferred offshore by eddies is the primary means by which the ocean interior (22°S–34°S and east of 107°E) is warmed and the Leeuwin Current cooled. The Leeuwin Current jet and the eddies allow air–sea fluxes to transfer over 40 W m^{-2} of heat to the atmosphere in the southeast Indian Ocean.
Citation: Domingues, C. M., S. E. Wijffels, M. E. Maltrud, J. A. Church, and M. Tomczak (2006), Role of eddies in cooling the Leeuwin Current, *Geophys. Res. Lett.*, *33*, L05603, doi:10.1029/2005GL025216.

1. Introduction

[2] Eastern boundaries of subtropical oceans are regions of surface equatorward currents and ocean heat gain, except in the South Indian Ocean where the Leeuwin Current (LC) flows poleward from the tropics to the subtropics [*Cresswell and Golding*, 1980] and where heat is lost to the atmosphere [*Doney et al.*, 1998]. In addition, the warm and relatively fresh waters of the LC sustain a variety of tropical marine species in temperate latitudes [*Saville-Kent*, 1897], a deep chlorophyll maximum (T. S. Moore et al., Phytoplankton variability off the western Australian coast: Mesoscale eddies and their role in cross-shelf exchange, submitted to *Deep-Sea Research, Part II*, 2005) and low tonnage, high value fisheries along the west Australian coast [*Caputi et al.*, 1996].

[3] The LC has a clear seasonal cycle and ENSO related variability [*Feng et al.*, 2003]. The warmest and strongest poleward flow of tropical waters occurs in May–June, and the current is warmer and stronger during La Niña years than in El Niño years. Little is known about the variability of its equatorward undercurrent, the Leeuwin Undercurrent (LUC) [*Thompson*, 1984]. Mesoscale eddies are an intrinsic part of the system [*Legeckis and Cresswell*, 1981] and their eddy kinetic energy (EKE) is the strongest of all the eastern boundaries [*Feng et al.*, 2005]. Although a variety of mesoscale features are evident in satellite imagery (http://www.marine.csiro.au/remotesensing/oceancurrents/), the most impressive are the large and long lived warm core vortices which detach from the boundary flow of the LC and migrate westward, transferring heat into the southeast Indian Ocean Subtropical Gyre [*Fang and Morrow*, 2003].

[4] The observed 5°C cooling of the LC along the west Australian coast [*Ridgway and Condie*, 2004], from North West Cape (22°S) to Cape Leeuwin (34°S), is thought to arise from some combination of air-sea and eddy heat fluxes and of seasonal and interannual rectification of currents and temperatures. Here, we perform a heat budget analysis using monthly averaged output from a 0.28° resolution global model to quantitatively determine which processes lead to the cooling of the LC for the region between 22°S and 34°S.

2. Model Description

[5] The numerical simulation used is the Los Alamos National Laboratory POP11B global ocean circulation model (77°N–77°S), with ~31 km (0.28°) horizontal resolution at the equator which decreases to ~6.5 km at the highest latitudes, 20 vertical levels, 9 in the upper 500 m, spanning from January 1993 to December 1997 [*Maltrud et al.*, 1998; *Garfield et al.*, 2001]. POP11B was forced with the European Centre for Medium–range Weather Forecasting (ECMWF) daily 10-m wind stresses. The model surface heat fluxes were a sum of the monthly climatological ECMWF fluxes [*Barnier et al.*, 1995] and a relaxation (with a spatially varying timescale) to an effective sea surface temperature. Freshwater fluxes were parameterised by restoring the surface salinity to a monthly climatology [*Levitus*, 1982] with a 1-month relaxation timescale. POP11B qualitatively reproduces the observed mean state, low–frequency variability and hydrographic structure of the upper southeast Indian Ocean [*Domingues*, 2005]. It features a vigorous eddy field off Western Australia though the model sea surface height variability and EKE are about 30–40% lower than altimetry data (M. Feng, personal communication, 2006). In addition, the model EKE appears to decay offshore somewhat more rapidly than in the real ocean (M. Feng, personal communication, 2006). Further details on the model's formulation and performance are found in *Maltrud et al.* [1998].

3. Method

[6] Heat budgets (Table 1) have been calculated for two regions (Figure 1), from the surface to the ocean bottom and

[1]Marine and Atmospheric Research, Commonwealth Scientific and Industrial Research Organisation, Hobart, Tasmania, Australia.
[2]School of Chemistry, Physics and Earth Sciences, Flinders University, Adelaide, South Australia, Australia.
[3]Fluid Dynamics Group, Los Alamos National Laboratory, Los Alamos, New Mexico, USA.

0094-8276/06/2005GL025216

Table 1. Heat Balance of the Coastal and Offshore Boxes Based on Two Depth Integrations, 0–185 m to Roughly Represent Leeuwin Current Depths and Full Depth (0–5200 m) to Represent the Entire Water Column[a]

Heat Budget	Box			
	Offshore		Coastal	
Surface flux, TW	−30	−30	−12	−12
Depth integration, m	0–185	0–5200	0–185	0–5200
$\nabla\cdot\langle \boldsymbol{U}\Theta\rangle$, TW	31	30	12	11
$\nabla\cdot(\langle \boldsymbol{U}\rangle\langle\Theta\rangle)$, TW	17	8	40	54
$\nabla\cdot\langle \boldsymbol{U}'\Theta'\rangle$, TW	14	22	−28	−43
Box surface area, 10^{12} m^2	0.80	0.80	0.24	0.24

[a]Heat fluxes into ocean boxes are positive.

also from the surface to 185 m. The shallower integration depth approximately separates the poleward flow of the LC from the deeper equatorward flow of the LUC. The coastal box encompasses the main jet of the LC and shelf waters whereas the offshore box includes part of the Subtropical Gyre east of 107°E, where one finds a highly energetic mesoscale field [*Feng et al.*, 2005] embedded in a series of narrow near surface eastward and deeper westward jets (C. M. Domingues et al., Simulated Lagrangian patterns of the large scale ocean circulation of the Leeuwin Current System off Western Australia, submitted to *Deep-Sea Research, Part II*, 2005). A regional overview of the heat balance is further obtained by analysing a series of 1° × 1° boxes within the study area in the upper 185 m. For each box, the residual (storage and diffusion) between the net surface heat flux and the divergence of the total advective ocean heat transport is small for the model 5-year averaged heat balance (not shown).

[7] A Reynolds decomposition is used to separate the total advective ocean heat transport (actually temperature transport relative to 0°C) into its 5-year mean and perturbations at seasonal, interannual and eddy timescales (equation (1)). The total heat flux, $\langle \boldsymbol{U}\Theta\rangle$, and its transport by the mean flow, $\langle \boldsymbol{U}\rangle\langle\Theta\rangle$, are calculated from the stored monthly average values of velocity, heat (see below) and heat flux. The heat flux associated with the seasonal values, $\langle \boldsymbol{U}_s'\Theta_s'\rangle$, have been calculated from monthly average deviations from the 5-year average and the interannual flux, $\langle \boldsymbol{U}_i'\Theta_i'\rangle$, from deviations from both the 5-year mean and 5-year monthly averages. Cross−products at these two timescales, $\langle \boldsymbol{U}_s'\Theta_i'\rangle$ and $\langle \boldsymbol{U}_i'\Theta_s'\rangle$, have also been formed. The eddy term, $\langle \boldsymbol{U}'\Theta'\rangle$, has been determined as the residual of the above components of the heat budget (equation (1)) as only monthly averages are available, and is due to correlations at submonthly timescales.

$$\langle U\Theta\rangle = \langle U\rangle\langle\Theta\rangle + \langle U_s'\Theta_s'\rangle + \langle U_i'\Theta_i'\rangle + \langle U_s'\Theta_i'\rangle + \langle U_i'\Theta_s'\rangle + \langle U'\Theta'\rangle \quad (1)$$

[8] Here, $\boldsymbol{U}$ is the velocity; Θ is heat ($\rho Cp\theta$, in which ρ = 1025 kg m^{-3}, Cp = 3989 J kg^{-1} °C^{-1}) and θ is potential temperature), $\langle\ \rangle$ denote 5-year average and primes are deviations at seasonal (s), interannual (i) and submonthly timescales. To calculate divergences, the heat budget components were integrated along the sides and bottom faces of the boxes.

4. Heat Budgets

[9] The southeast Indian Ocean off Western Australia releases a considerable amount of heat to the overlying atmosphere (Figure 1a). The ocean heat loss is largest within the coastal box (−50 to −70 W m^{-2}), along the mean path of the LC as inferred from the upper 185 m potential temperature tongue (Figure 1b) and the poleward heat transport vectors (Figure 1c). It is also large in locations adjacent to the LC's outer edge where mesoscale eddies are highly active. Away from the coastal boundary, the ocean heat loss gradually tapers to −20 W m^{-2} near the western rim of the offshore box. This regional cooling in POP11B is in quite good agreement with observations. Over the study area, the model surface fluxes integrate to −42 W m^{-2} while observational fluxes from the Southampton Oceanographic Centre [*Josey et al.*, 1999] are about 50% larger at −67 W m^{-2}.

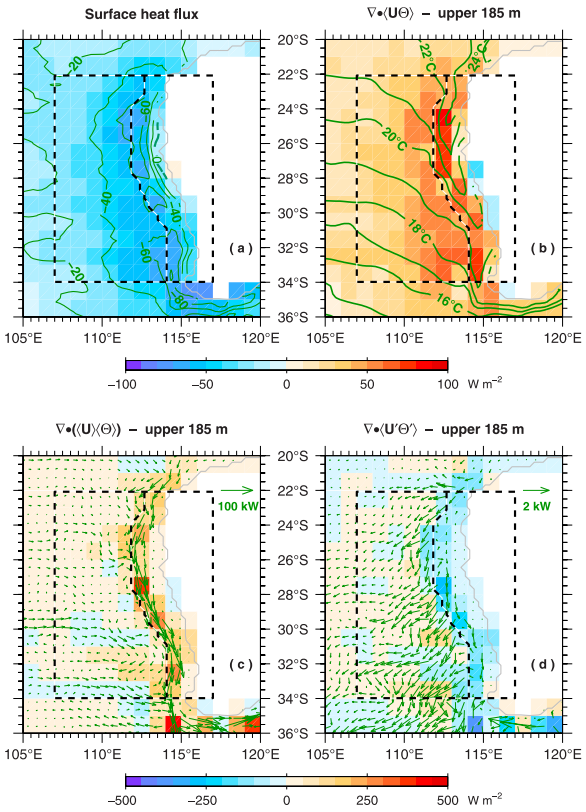

Figure 1. Elements of the ocean heat balance in the upper 185 m of the southeast Indian Ocean in a series of 1° × 1° grid boxes as calculated from the POP11B 1993/97 model simulation: (a) surface heat flux, (b) total ocean heat divergence and mean potential temperature (green contours), (c) mean ocean heat divergence and mean temperature fluxes referenced to 0°C, and (d) eddy ocean heat divergence and eddy temperature fluxes referenced to 0°C. Ocean heat loss is negative. The thick dashed black line denotes the boundaries of the coastal and offshore boxes used in the heat budget listed in Table 1. The line in gray represents the coastline.

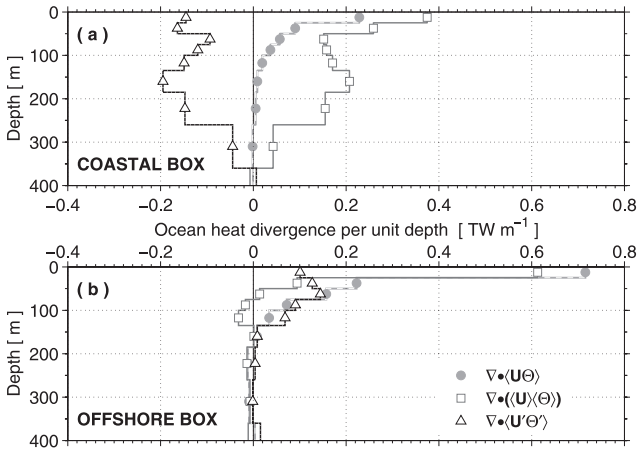

Figure 2. Total, mean and eddy ocean heat divergence per unit depth in the upper 400 m, for the (a) coastal box and (b) offshore box.

[10] The heat balance in both coastal and offshore boxes is primarily between the surface flux, the mean ($\nabla\cdot(\langle \boldsymbol{U}\rangle\langle\Theta\rangle)$) and the eddy ($\nabla\cdot\langle \boldsymbol{U}'\Theta'\rangle$) divergence terms in the two depth integrations (Table 1). The mean and eddy heat divergences are greatest in the top 300 m within the coastal box (Figure 2a), at depths of both the LC and LUC. As these two terms balance each other, their vertical profiles tend to be a mirror image except in the model mixed layer where the surface flux produces ocean cooling. The "storage+diffusion" terms and the seasonal and interannual terms, including their cross–products, are all small (not shown). Even though the seasonal and interannual variability of the study area has been well captured by POP11B [*Domingues*, 2005], rectification on those timescales appears to play a small role in the mean heat balance.

[11] In the coastal box, the large mean heat convergence (40 TW) in the upper 185 m is balanced by the eddy divergence (−28 TW) and the surface flux (−12 TW; Table 1). Thus the eddy divergence explains about 70% of the cooling of the mean jet of the LC while the local air-sea fluxes play a lesser role. In the full depth integration, the eddy heat divergence (−43 TW) accounts for about 80% of the cooling of the entire water column in that coastal region. Mean and eddy flows also dominate the heat balance of the upper LUC (185–300 m, Figure 2a), respectively warming and cooling the LUC along its equatorward path.

[12] In the offshore box, the ocean is warmed by both the convergence of mean (17 TW) and eddy (14 TW) fluxes in the top 185 m (Table 1) and cooled at the surface through air-sea fluxes (−30 TW). Significant mean heat convergence only occurs in the top 75 m (Figure 2b). Below 185 m, the ocean is warmed by eddy convergence (22 – 14 = 8 TW) and almost equally cooled by mean divergence (8 – 17 = −9 TW). The eddy heat convergence (22 TW) accounts for about 70% of the warming of the full depth offshore region. Only about half of the 43 TW (Table 1) removed from the coastal box by eddies warms the Subtropical Gyre east of 107°E, while the other half is transferred to the south of 34°S and to the west of 107°E (Figure 1d).

[13] Thus, the heat removed from the mean jet of the LC by eddy fluxes, particularly within some hot spots along the outer edge of the current, is spread offshore in a broadly coherent southwestward direction (Figure 1d), that is down the mean temperature gradient. This offshore spreading of heat allows the air–sea fluxes to cool the ocean over a much larger area (Figure 1a) and emphasizes the importance of lateral exchange between boundary and ocean interior.

5. Westward Eddy Heat Flux

[14] Using *Feng et al.'s* [2005] pointwise westward eddy heat flux (WEHF) of 3.2×10^7 W m^{-1} over the 0–200 depth, from mooring array data at 29°S, and integrating over ∼1350 km, from North West Cape (22°S) to Cape Leeuwin (34°S), with and without their 50% factor to account for spatial variations of the eddy field along the west Australian coast, we obtain 22–44 TW. If we integrate the upper 200 m WEHF in the model, along the outer edge of the coastal box, from 22°S to 34°S, we obtain 28 TW. If we compute the WEHF from a model grid point close to the mooring array, our model value is about half of Feng et al.'s. So, despite the eddy permitting nature of POP11B and associated lower levels of EKE and the difficulty of comparing point estimates in noisy fields like eddy heat fluxes, the model's WEHF estimates are of the same order of magnitude as obtained from Feng et al.'s observations.

[15] From a combination of in situ and altimeter data, *Morrow et al.* [2003] estimate an annual average WEHF of only 5 TW, associated with large and long lived warm core eddies in the upper 2500 m. These coherent eddies detach from the boundary flow of the LC and move toward the ocean interior, preferentially northwestward along isothermal corridors [*Fang and Morrow*, 2003]. Morrow et al.'s WEHF estimate is much smaller than the model WEHF of 43 TW, integrated for the same depth range, and the 22–44 TW WEHF calculated from Feng et al.'s observations. Although warm core coherent eddies are seen to propagate in a similar fashion in the model to the observations of *Fang and Morrow* [2003], they are clearly not the major contribution to the WEHF. The WEHF is much larger and transports heat southwestward (Figure 1d), perpendicular to isotherms (Figure 1b). We cannot specify the submonthly processes generating the WEHF in POP11B with our heat budget analysis but we postulate they are primarily associated with the short lived ("transient") warm core eddies which also populate the ocean interior off Western Australia. These eddies are frequently formed and tend to decay quickly (east of 110°E) as they move westward–southwestward [*Fang and Morrow*, 2003]. Their pathways given by *Morrow et al.* [2004] (their Figure 1) are quite consistent with the broad southwestward spreading of the eddy heat flux shown in Figure 1d. Consequently, long lived warm core coherent eddies contribute to but do not dominate the LC's cooling.

6. Conclusions

[16] In the POP11B model, the primary mechanism cooling the LC between 22°S and 34°S is the divergence of the eddy heat fluxes associated with processes operating at submonthly timescales. Heat is advected poleward by the mean flow and then transferred westward to the adjacent offshore ocean by these eddy fluxes. The model westward eddy heat flux is in the same order of magnitude of observational values [*Feng et al.*, 2005], and we suggest

it is mainly associated with frequently formed and short lived warm core eddies.

[17] While the eddy heat fluxes originate in a narrow strip along the LC's edge, they radiate across isotherms to the southwest and "dump" their heat over a much broader area of the southeastern Indian Ocean. This effectively "smears" the lateral temperature gradients in the region. The broad wedge of warm water associated with the mean climatological LC is not maintained by a broad mean flow but by a narrow boundary jet diffusing heat laterally through eddy fluxes.

[18] The full depth-integrated eddy heat flux transfer from the coast to the ocean interior is responsible for 70% of the warming of a vast area of the southeastern Indian Ocean east of 107°E – the other 30% is accounted by the mean convergence – over which the local air-sea fluxes extract heat. The far reaching influence of the narrow LC jet and the eddies generated by the LC may be difficult to simulate accurately in lower resolution climate models that assume a local eddy parameterization in which the eddy flux divergence is related to the local mean flow. Nevertheless it is worth noting that in POP11B the eddy heat flux does appear to have a significant downgradient component perpendicular to the mean isotherms, and therefore at least part of it may be amenable to standard parameterization techniques in climate models.

[19] Despite POP11B's possible shortcomings (e.g., lower levels of EKE and surface flux inaccuracies), the results obtained from our heat budget analysis provide a robust picture about the relative role of eddies and surface fluxes in the cooling of the LC. The model results show the LC to be a very leaky pipe, highly connected to the ocean interior via eddy fluxes. Eddies, and not local air-sea fluxes, drive the current's property changes, especially below the mixed layer. Therefore eddies are not just key to the LC momentum balance as shown by *Feng et al.* [2005] but they are also critical for its heat balance. Salinity patterns also support this view [*Domingues*, 2005].

[20] **Acknowledgments.** C. Domingues was supported by the Brazilian Research Council (CNPq, grant 200412/97-3). M. Maltrud performed the POP simulations under the auspices of the U.S. Department of Energy Office of Science. We would like to thank the two reviewers for their valuable constructive comments. This paper is a contribution to the CSIRO Climate Change Research Program and was funded in part by Australia's Climate Change Science Program and Australia's National Greenhouse Program.

References

Barnier, B., L. Siefridt, and P. Marchesiello (1995), Thermal forcing for a global ocean circulation model using a three-year climatology of ECMWF analyses, *J. Mar. Syst.*, *6*, 363–380.

Caputi, N., W. J. Fletcher, A. Pearce, and C. F. Chubb (1996), Effect of the Leeuwin Current on the recruitment of fish and invertebrates along the western Australian coast, *Mar. Freshwater Res.*, *47*, 147–155.

Cresswell, G. R., and T. J. Golding (1980), Observations of a south-flowing current in the southeastern Indian Ocean, *Deep-Sea Res., Part A*, *27*, 449–466.

Domingues, C. M. (2005), Kinematics and heat budget of the Leeuwin Current, Ph.D. dissertation, 156 pp., Flinders Univ., Adelaide, S. Aust., Australia.

Doney, S. C., W. G. Large, and F. O. Bryan (1998), Surface ocean fluxes and water mass transformation rates in the coupled NCAR climate system model, *J. Clim.*, *11*, 1420–1441.

Fang, F., and R. Morrow (2003), Evolution, movement and decay of warm-core Leeuwin Current eddies, *Deep-Sea Res., Part II*, *50*, 2245–2261.

Feng, M., G. Meyers, A. Pearce, and S. Wijffels (2003), Annual and interannual variations of the Leeuwin Current at 32°S, *J. Geophys. Res.*, *108*(C11), 3355, doi:10.1029/2002JC001763.

Feng, M., S. Wijffels, S. Godfrey, and G. Meyers (2005), Do eddies play a role in the momentum balance of the Leeuwin Current?, *J. Phys. Oceanogr.*, *35*, 964–975.

Garfield, N., M. E. Maltrud, C. A. Collins, T. A. Rago, and R. G. Paquette (2001), Lagrangian flow in the California Undercurrent, an observation and model comparison, *J. Mar. Syst.*, *29*, 201–220.

Josey, S. A., E. C. Kent, and P. K. Taylor (1999), New insights into the ocean heat budget closure problem from analysis of the SOC air-sea flux climatology, *J. Clim.*, *12*, 2856–2880.

Legeckis, R., and G. R. Cresswell (1981), Satellite observations of sea surface temperature fronts off the coast of western and southern Australia, *Deep-Sea Res.*, *28*, 297–306.

Levitus, S. (1982), *Climatological Atlas of the World Ocean*, *NOAA Prof. Pap. 13*, 173 pp., U. S. Govt. Print. Off., Washington, D. C.

Maltrud, M. E., R. D. Smith, A. J. Semtner, and R. C. Malone (1998), Global eddy-resolving ocean simulations driven by 1985–1995, *J. Geophys. Res.*, *103*, 30,825–30,853.

Morrow, R., F. Fang, M. Fieux, and R. Molcard (2003), Anatomy of three warm-core Leeuwin Current eddies, *Deep-Sea Res. II*, *50*, 2229–2243.

Morrow, R., F. Birol, D. Griffin, and J. Sudre (2004), Divergent pathways of cyclonic and anti-cyclonic ocean eddies, *Geophys. Res. Lett.*, *31*, L24311, doi:10.1029/2004GL020974.

Ridgway, K. R., and S. A. Condie (2004), The 5500-km-long boundary flow off western and southern Australia, *J. Geophys. Res.*, *109*, C04017, doi:10.1029/2003JC001921.

Saville-Kent, W. (1897), *The Naturalist in Australia*, 302 pp., CRC Press, Boca Raton, Fla.

Thompson, R. O. R. Y. (1984), Observations of the Leeuwin Current off Western Australia, *J. Phys. Oceanogr.*, *14*, 623–628.

J. A. Church, C. M. Domingues, and S. E. Wijffels, Marine and Atmospheric Research CSIRO, GPO Box 1538, Hobart, TAS 7001, Australia. (john.church@csiro.au; catia.domingues@csiro.au; susan.wijffels@csiro.au)

M. E. Maltrud, Fluid Dynamics Group, Los Alamos National Laboratory (T–3), MS B216, Los Alamos, NM 87545, USA. (maltrud@lanl.gov)

M. Tomczak, School of Chemistry, Physics and Earth Sciences, Flinders University, GPO Box 2100, Adelaide, SA 5001, Australia. (matthias.tomczak@flinders.edu.au)